







# Bacteria-Oil Microaggregates Are an Important Mechanism for Hydrocarbon Degradation in the Marine Water Column

 Amanda M. Achberger,<sup>a</sup>  Shawn M. Doyle,<sup>a</sup> Makeda I. Mills,<sup>a</sup> Charles P. Holmes II,<sup>a</sup>  Antonietta Quigg,<sup>a,b</sup>  Jason B. Sylvan<sup>a</sup>

<sup>a</sup>Department of Oceanography, Texas A&M University, College Station, Texas, USA

<sup>b</sup>Department of Marine Biology, Texas A&M University-Galveston, Galveston, Texas, USA

**ABSTRACT** Following oil spills in aquatic environments, oil-associated flocculants observed within contaminated waters ultimately lead to the sedimentation of oil as marine oil snow (MOS). To better understand the role of aggregates in hydrocarbon degradation and transport, we experimentally produced a MOS sedimentation event using Gulf of Mexico coastal waters amended with oil or oil plus dispersant. In addition to the formation of MOS, smaller micrometer-scale (10- to 150- $\mu$ m) microbial aggregates were observed. Visual inspection of these microaggregates revealed that they were most abundant in the oil-amended treatments and frequently associated with oil droplets, linking their formation to the presence of oil. The peak abundance of the microaggregates coincided with the maximum rates of biological hydrocarbon oxidation estimated by the mineralization of <sup>14</sup>C-labeled hexadecane and naphthalene. To elucidate the potential of microaggregates to serve as hot spots for hydrocarbon degradation, we characterized the free-living and aggregate-associated microbial assemblages using 16S rRNA gene sequencing. The microaggregate population was found to be bacterially dominated and enriched with putative hydrocarbon-degrading taxa. Direct observation of some of these taxa using catalyzed reporter deposition fluorescence *in situ* hybridization confirmed their greater abundance within microaggregates relative to the surrounding seawater. Metagenomic sequencing of these bacteria-oil microaggregates (BOMAs) further supported their community's capacity to utilize a wide variety of hydrocarbon compounds. Taken together, these data highlight that BOMAs are inherent features in the biological response to oil spills and likely important hot spots for hydrocarbon oxidation in the ocean.

**IMPORTANCE** Vast quantities of oil-associated marine snow (MOS) formed in the water column as part of the natural biological response to the Deepwater Horizon drilling accident. Despite the scale of the event, uncertainty remains about the mechanisms controlling MOS formation and its impact on the environment. In addition to MOS, we observed micrometer-scale (10- to 150- $\mu$ m) aggregates whose abundance coincided with maximum rates of hydrocarbon degradation and whose composition was dominated by hydrocarbon-degrading bacteria with the genetic potential to metabolize a range of these compounds. This targeted study examining the role of these bacteria-oil microaggregates in hydrocarbon degradation reveals details of this fundamental component of the biological response to oil spills, and with it, alterations to biogeochemical cycling in the ocean.

**KEYWORDS** marine oil snow, microbial aggregate, hydrocarbon degradation

**F**orecasting the fate of marine oil spills depends on a mechanistic understanding of the various oil biodegradation and transport processes which occur in the ocean. The role of microorganisms in marine oil spill response has been a topic of major research in the last decade (1–6). Such work has yielded significant progress in

**Citation** Achberger AM, Doyle SM, Mills MI, Holmes CP, II, Quigg A, Sylvan JB. 2021. Bacteria-oil microaggregates are an important mechanism for hydrocarbon degradation in the marine water column. *mSystems* 6:e01105-21. <https://doi.org/10.1128/mSystems.01105-21>.

**Editor** Zarath M. Summers, ExxonMobil Research and Engineering

**Copyright** © 2021 Achberger et al. This is an open-access article distributed under the terms of the [Creative Commons Attribution 4.0 International license](https://creativecommons.org/licenses/by/4.0/).

Address correspondence to Amanda M. Achberger, [a.m.achberger@gmail.com](mailto:a.m.achberger@gmail.com), or Jason B. Sylvan, [jasonsylvan@tamu.edu](mailto:jasonsylvan@tamu.edu).

**Received** 7 September 2021

**Accepted** 15 September 2021

**Published** 5 October 2021

determining the composition, function, and activity of the water column microbial community involved in hydrocarbon pollution remediation. A few such studies have noted the presence of small clusters of aggregated cells with diameters of  $<500 \mu\text{m}$ , here called microaggregates (1, 7–10). One of these studies found a correlation between oil concentration and microaggregate abundance, linking their formation to the presence of oil (10). Despite their potential importance, little research has been conducted focusing on microaggregates, and thus, their impact on the transport and degradation of hydrocarbons following a spill is largely unknown.

In contrast, the importance of macroscale marine oil snow (MOS) sedimentation and flocculent accumulation (MOSSFA) events (11, 12) in determining the fate of spilled oil has recently garnered much attention. The 2010 Deepwater Horizon (DwH) oil spill in the Gulf of Mexico demonstrated that marine snow can transport enormous amounts of oil to the seafloor through the formation of large ( $\geq 500\text{-}\mu\text{m}$ ), mucus-rich, oil-associated aggregates (11–14). It is believed that this MOSSFA event was a direct result of the production of exopolymeric substances (EPS) by phytoplankton and bacteria exposed to oil (7, 13). Numerous marine microorganisms have been shown to produce EPS that can serve as biosurfactants that emulsify hydrocarbons and enhance their biodegradability (15, 16). EPS also provide a “sticky” matrix that can promote the aggregation of microorganisms with oil droplets suspended in the water column (1, 13, 17, 18).

This type of biological response was not unique to the DwH spill. Evidence for MOS events was also documented following the 1977 Tsesis oil spill in Sweden (19) and the 1979 Ixtoc I oil spill in the southern Gulf of Mexico (20). Although microaggregates are too small to formally be considered MOS, their correlation with elevated oil concentrations has led some to speculate that they are possible precursors to MOS formation (10). Despite the growing appreciation for the importance of MOS after an oil spill, we still lack a full understanding of what role microaggregates might serve in such a process or how the degradation of oil incorporated into aggregates differs from that of oil dispersed freely into the water column.

To better explain and predict the fate of oil spilled in the ocean, it is critical to understand the mechanisms of microaggregate formation and their significance in the natural bioremediation of hydrocarbon pollution. In this study, we utilized mesocosm experiments to assess the behavior of microaggregates under control conditions (sea-water only) and in the presence of oil. Given the widespread use of dispersants for oil spill remediation, which not only alter the size and abundance of suspended oil droplets but may also impact the aggregation process (21–23), we also tested the effects of chemically dispersed oil. We present data on microaggregate formation (counts, size) as well as a description of their microbial community structure using 16S rRNA gene amplicon sequencing and catalyzed reporter deposition fluorescence *in situ* hybridization (CARD-FISH). We further evaluated the microbial community's potential for hydrocarbon degradation through metagenomic sequence analysis and radiotracer ( $^{14}\text{C}$ -labeled hexadecane and naphthalene) assays. Our results show the establishment of bacterially dominated microaggregate specific communities and a link between their formation and abundance with hydrocarbon degradation. Furthermore, this work reveals that these bacteria-oil microaggregates (BOMAs) are an important mechanism for hydrocarbon degradation and transport in the water column.

## RESULTS

**Microbial degradation of hydrocarbons.** The initial concentration of hydrocarbons in the mesocosms, measured as estimated oil equivalents (EOEs), was statistically the same ( $P$  value = 0.13) in the oil-only and oil-plus-dispersant treatments: 2.15 ( $\pm 0.12$ ) and 2.62 ( $\pm 0.18$ ) mg/liter, respectively (Fig. 1A). This allows us to evaluate the dispersant's effects on the microaggregates and microbial communities without the confounding influence of variable oil concentrations between treatments. Over the next 8 days, a decrease in the concentration following first-order decay kinetics occurred after which

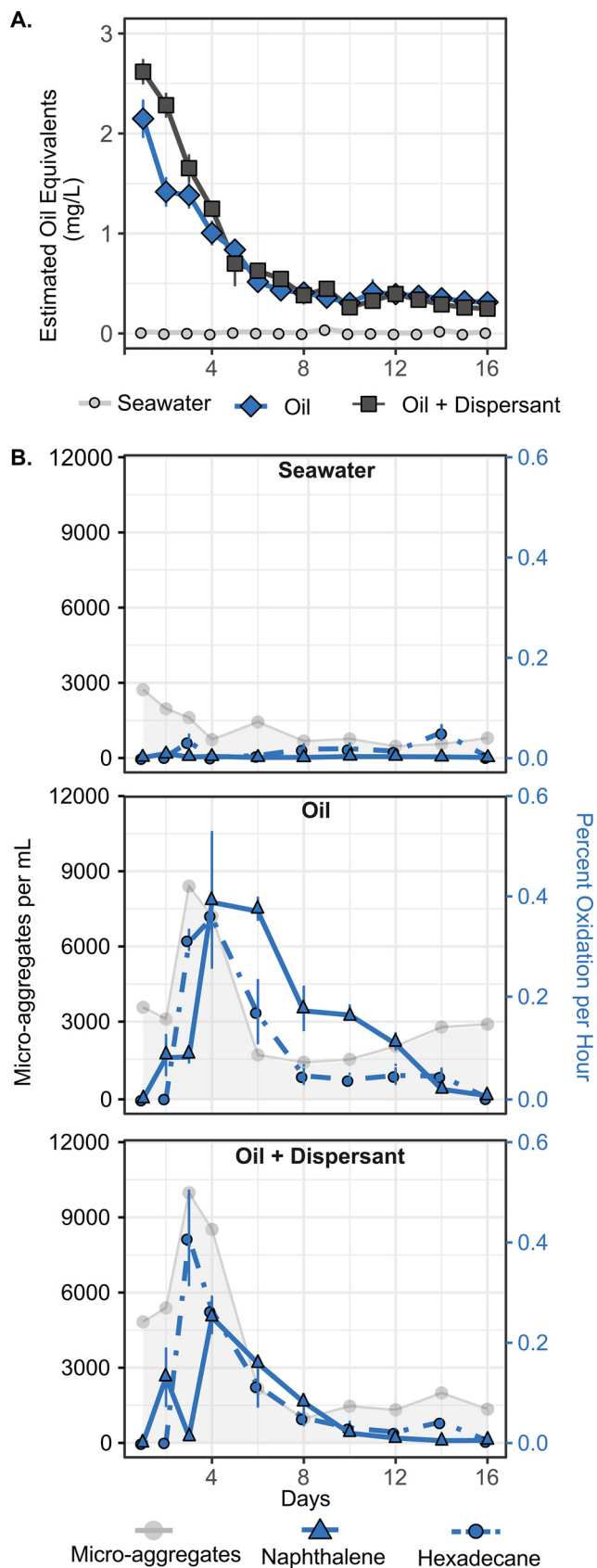


**FIG 1** Hydrocarbon degradation over time. (A) Oil concentration expressed as estimated oil equivalents (previously reported by reference 24). (B) Microaggregate abundance is shown as (Continued on next page)

the concentrations remained stable between 0.25 and 0.45 mg/liter for the duration of the experiment (16 days [24]). The decreasing ratios of  $n\text{-C}_{17}$ /pristane and  $n\text{-C}_{18}$ /phytane over time indicated that a portion of this loss was attributable to biodegradation (see Fig. S1 in the supplemental material) (24). A low but detectable background of hydrocarbons was measured in the seawater control samples that showed no significant change with time (Fig. 1A). Further discussion of individual hydrocarbon components and a detailed account of their degradation rates are presented elsewhere (24).

Cell abundance was similar in all treatments at the start of the experiment ( $\sim 6 \times 10^5$  cells/ml) and increased to  $\sim 2 \times 10^6$  cells/ml after 16 days (Fig. S2). No treatment had statistically different cell concentrations over the entire experiment. Similar trends in cell abundances were noted in previous mesocosm experiments simulating oil spills in surface seawater (10, 25). Microaggregates consisting of tens to hundreds of cells were present in the freshly collected seawater used to establish the mesocosms at *in situ* concentrations of  $\sim 4,400$  microaggregates/ml. While the abundance of these microaggregates decreased over time in the seawater control, their abundance in the oil-only and oil-plus-dispersant treatments increased by  $\geq 100\%$  by day 3 before also slowly declining (Fig. 1B). Throughout much of the experiment, more microaggregates were observed in the dispersed oil treatment than in the treatment amended with just oil (Fig. 1B). Within both oil-amended treatments (dispersed and oil-only),  $>85\%$  of microaggregates examined had visible droplets of oil incorporated into their structure, and eukaryotic cells, such as phytoplankton, were rarely observed. There was no consistent difference in the size distribution of the microaggregates between treatments or over time with the exception of microaggregates in the seawater control after day 12 (Fig. S3).

Biological rates of hydrocarbon oxidation were estimated based on the conversion of the C1 carbon of model alkane ( $[1\text{-}^{14}\text{C}]$ hexadecane) and polycyclic aromatic hydrocarbon (PAH;  $[1\text{-}^{14}\text{C}]$ naphthalene) compounds to  $[^{14}\text{C}]$ carbon dioxide (Fig. 1B). After an initial 24-h lag, hexadecane oxidation rates sharply increased, reaching maximum rates of degradation on day 3 in oil plus dispersant and days 4 to 5 in oil-only treatments. Despite this slight difference in the timing of peak rates, there was no statistical difference in hexadecane oxidation rates between the two oil-amended treatments ( $P \geq 0.10$ ) over the course of the experiment. In both oil-only and oil-plus-dispersant treatments, naphthalene oxidation rates reached their maximum on day 4. Higher oxidation rates were measured in the oil-only samples than in oil plus dispersant through much of the experiment (days 3, 6, and 10 to 14;  $P < 0.02$ ). Low rates of hexadecane oxidation were measured in the seawater control tanks on day 3 and during the second half of the experiment (days 8 to 14); however, naphthalene oxidation in the seawater control was never above background.

**Microaggregate-associated communities.** Microbial community composition in size-fractionated samples ( $>3.0 \mu\text{m}$  and  $0.2$  to  $3.0 \mu\text{m}$ ) was assessed via analysis of 16S rRNA gene amplicon sequencing variants (ASVs). Microscopic examination of size-fractionated samples ( $n = 3$ ) revealed that nearly all microaggregates were retained on the  $3.0\text{-}\mu\text{m}$  filters. Therefore, cells on the  $3.0\text{-}\mu\text{m}$  filter were considered microaggregate associated, although a small number of free-living cells ( $<5\%$ ) were sometimes also observed to be present in this size fraction via visual inspection under a microscope. A nonmetric multidimensional scaling (NMDS) analysis of community structure revealed that, at the start of the experiment, microaggregate-associated communities ( $>3.0 \mu\text{m}$ ) were distinct from free-living ( $0.2$  to  $3.0 \mu\text{m}$ ) communities regardless of treatment (Fig. S4). Between days 3 and 8, this structure began to noticeably diverge based on treatment such that by the end of the experiment, the communities within treatments were most similar to each other despite size fractionation.

#### FIG 1 Legend (Continued)

microaggregates per milliliter (left axis). Oxidation rates of  $[^{14}\text{C}]$ hexadecane and  $[^{14}\text{C}]$ naphthalene (right axis), respectively, are shown for each treatment group as a percentage of total available substrate oxidized per hour.

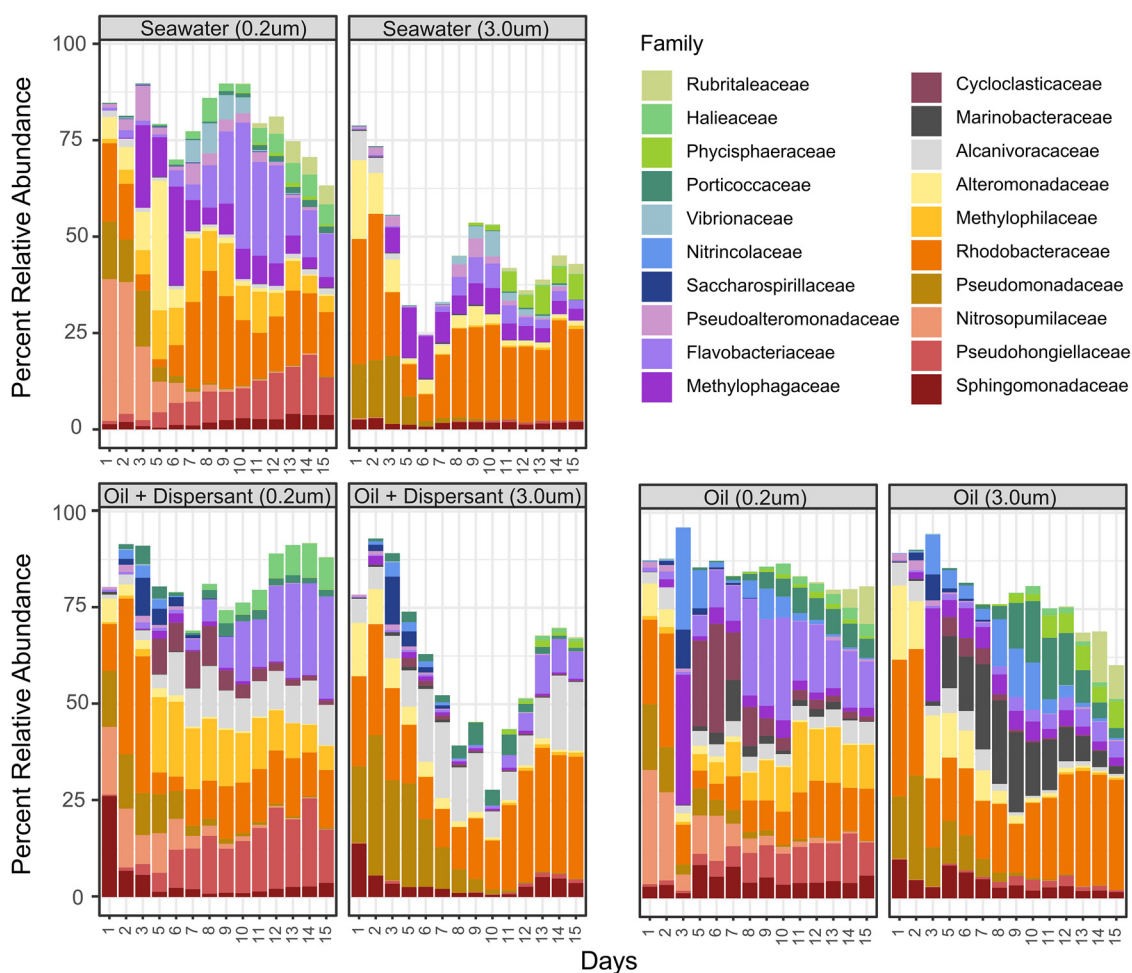


**FIG 2** Microbial community composition as assessed via PCR amplicon analysis of the V4 region of the 16S rRNA gene. The community's taxonomic distribution is described at the family level. Only the 20 most abundant families are shown.

On days 1 and 2, microbial communities in all three treatments were predominantly composed of members of the *Pseudomonadaceae*, *Rhodobacteraceae*, *Alteromonadaceae*, *Alcanivoraceae*, and *Nitrosopumilaceae* (Fig. 2). By day 3, differences between the two oil-amended treatments and the seawater control were apparent. Compared to the seawater control, an increase in relative abundance by members of the *Nitrincolaceae*, *Saccharospirillaceae*, *Alcanivoraceae*, and *Cycloclasticaceae* occurred in both the oil-only and oil-plus-dispersant treatments, while *Marinobacteraceae* taxa were prevalent only in the oil-only treatment. By the latter half of the experiment, when hydrocarbons were largely depleted, the relative abundance of *Flavobacteriaceae*, *Phycisphaeraceae*, *Halieaceae*, and *Porticoccaceae* increased in all treatments. Additionally, members of the *Rubritaleaceae* were also present in the seawater control and oil-only treatments. Over the course of the experiment, several of these groups, such as *Cycloclasticaceae*, *Methylophilaceae*, *Pseudohongiellaceae*, *Flavobacteriaceae*, and *Nitrosopumilaceae*, were more abundant on the 0.2- to 3.0- $\mu\text{m}$  size fraction than on the  $>3.0\text{-}\mu\text{m}$  fraction, revealing significant differences in the microbial community composition of the microaggregate and free-living fractions (Fig. 2).

Within each treatment, a linear discriminant analysis (LDA) combined with effect size measurements (26) was used to identify which specific ASVs were statistically more abundant in either the microaggregates or the free-living community. While no ASV showed significantly different distribution over the entire length of the experiment, several ASVs such as *Rhodobacteraceae* (ASV7), *Alteromonas* (ASV17), *Aestuariibacter*

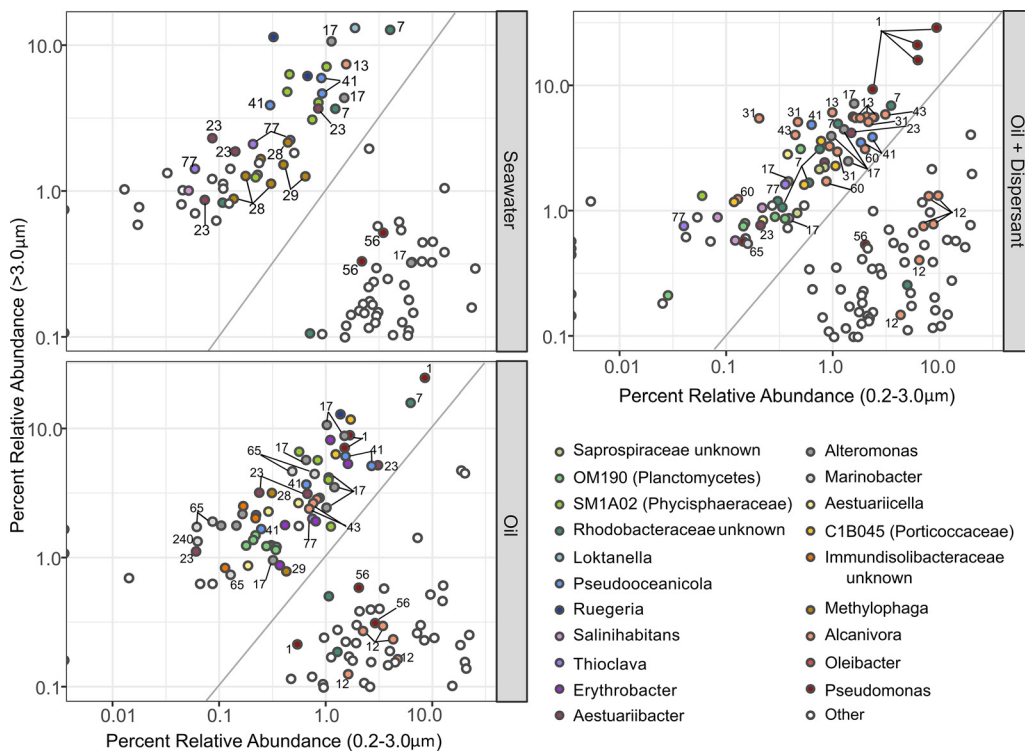


**FIG 3** Comparison of the microbial communities between aggregated and free-living groups for each treatment. Differential abundance analysis shows certain phylogenetic groups and ASVs are more abundant in either the >3.0- $\mu\text{m}$  (relative abundance on y axis) or 0.2- to 3.0- $\mu\text{m}$  (relative abundance on x axis) filter size fraction. The 20 most abundant genera are highlighted with all other less abundant genera as well as groups of unresolved phylogenetic affiliation denoted as other. ASVs of interest discussed in the main text are denoted with numbers within the graphs. A 1:1 ratio between the abundance of ASVs on the >3.0- and 0.2- to 3.0- $\mu\text{m}$  size fractions is depicted as a gray diagonal line within the graphs.

(ASV23), *Pseudoceanicola* (ASV41), and *Thioclava* (ASV77) were more abundant within the microaggregates regardless of treatment during the first 6 days (Fig. 3; Fig. S5). Several ASVs of *Alcanivorax* were statistically more abundant within the aggregated communities but showed different distribution patterns. For example, while *Alcanivorax* ASV13 was identified in every treatment, ASV43 was found only in the oil-amended samples and ASVs 31, 60, and 401 were notably more prevalent in microaggregates only in the oil-plus-dispersant treatments. Conversely, one ASV of *Alcanivorax* (ASV12) was more abundant in the free-living community and found in every treatment. A similar pattern was observed with other groups such as *Pseudomonas*: ASV1 was preferentially found among the aggregated community while ASV56 was detected in the free-living community. Additionally, some taxa, while detectable at low abundances in all treatments, showed a preference for certain conditions. For instance, ASVs of *Methylophaga* (ASV28 and ASV29) were often associated with microaggregates in the seawater control and oil-only treatments whereas ASVs of *Marinobacter* (ASV65 and ASV240) were predominantly only in the oil-only treatment.

Catalyzed reporter deposition-based fluorescence *in situ* hybridization (CARD-FISH) was used to verify the presence of *Alteromonas* sp. and *Alcanivorax* sp. in the microaggregates as suggested by the 16S rRNA gene analysis (Fig. 2 and Fig. S5). *Alteromonas*-related and *Alcanivorax*-related cells detected by the CARD-FISH probes were most often observed in microaggregate clusters rather than as free-living cells (Fig. S6A). However, there were also several free-living *Alcanivorax* targeted cells identified (Fig. S6B), which is in agreement with their overall distribution in the microbial community data as well as the LDA of ASVs, which confirmed that certain ASVs (e.g., ASV12) were prevalent in the 0.2- to 3.0- $\mu\text{m}$  fraction (Fig. 2 and 3).

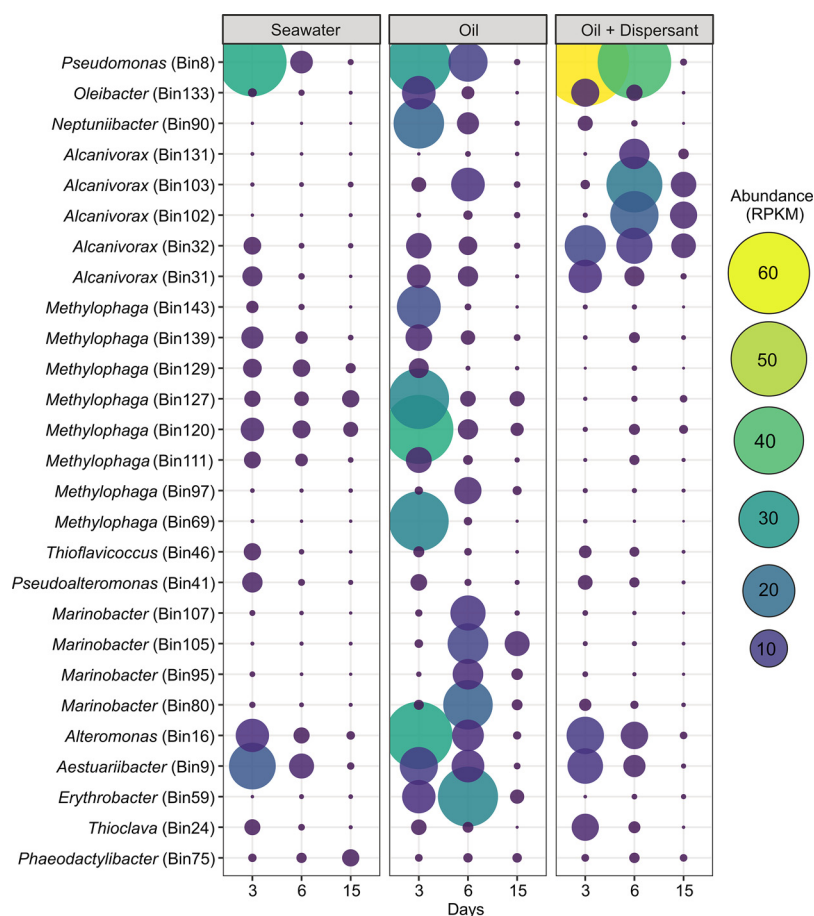


**FIG 4** Abundance of metagenome-assembled genomes (MAGs) in microaggregates expressed as reads per kilobase per million (RPKM). Statistics for individual MAGs are provided in Table S1.

**Microaggregate communities harbor genes for hydrocarbon degradation.** Based on the analysis of 16S rRNA genes in combination with hydrocarbon oxidation rates and microaggregate abundance profiles, major shifts in the microaggregate community structure and/or hydrocarbon degradation potential occurred on days 3, 6, and 15. Therefore, these days were chosen for metagenomic analysis of the microaggregate specific community ( $>3.0 \mu\text{m}$ ) to determine its genetic potential for hydrocarbon oxidation. From these samples, 27 quality metagenome-assembled genomes (MAGs,  $>50\%$  completion and  $<10\%$  contamination) were generated that were closely related to bacterial taxa identified as prevalent in microaggregates by the LDA of ASVs (Fig. 4 and Table S1). These MAGs were then searched for genes potentially involved in the degradation of hydrocarbon compounds and their intermediates. The identified genes were consolidated into three groups (alkane, aromatic, and fatty acid degradation; see reference 25). Alkane degradation includes hydroxylase and monooxygenase enzymes which convert alkanes into a fatty alcohol. This alcohol is then further oxidized by alcohol and aldehyde dehydrogenases to a fatty acid and enters the beta oxidation pathway as acyl coenzyme A (acyl-CoA). Because the genes involved in the conversion of the alcohol to a fatty acid and its subsequent breakdown are often involved in metabolisms unrelated to the degradation of alkanes, they were conservatively separated into the fatty acid degradation category. The aromatic degradation category includes enzymes involved in ring hydroxylation and cleavage as well as numerous multistep pathways needed for the continued breakdown of the resultant compounds.

On day 3 of the experiment, overall abundances of alkane, aromatic hydrocarbon, and fatty acid degradation genes were similar between treatments and largely

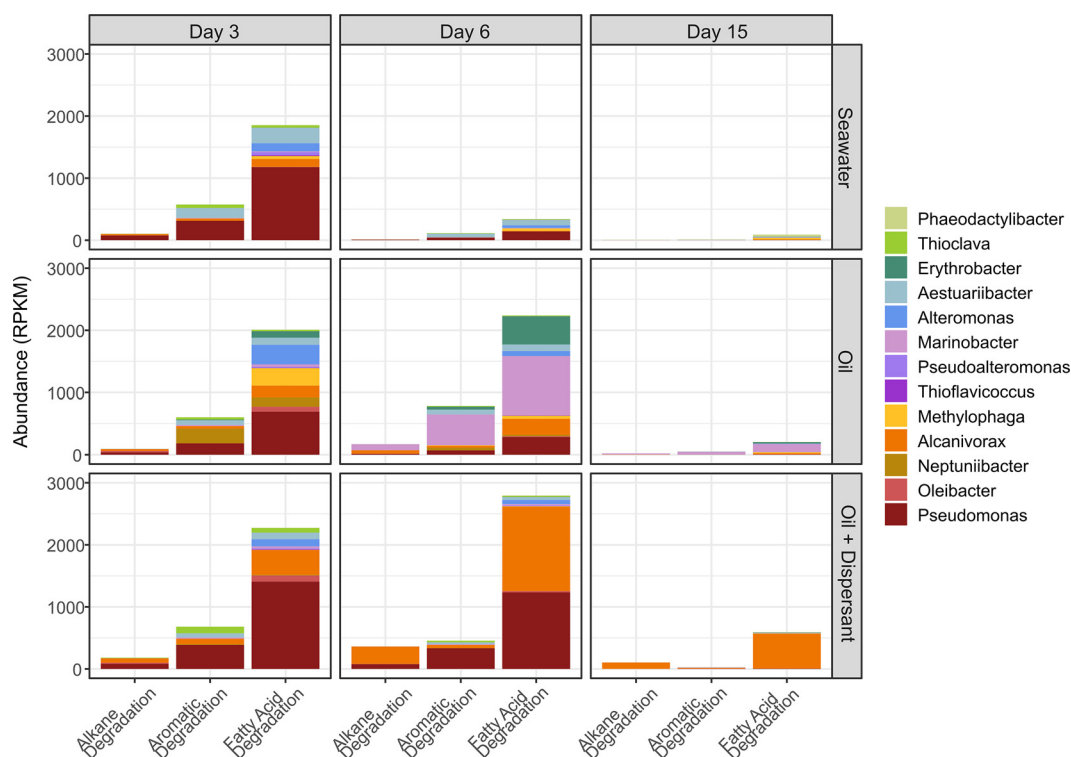


**FIG 5** Hydrocarbon degradation potential in metagenome-assembled genomes (MAGs) from taxa more abundant in microaggregates. Abundance of genes involved in the degradation of *n*-alkanes, PAHs, and fatty acids in MAGs.

belonged to a single abundant MAG of *Pseudomonas*, Bin 8 (Fig. 5). Genes for alkane degradation were also recovered from several MAGs of *Alcanivorax* (Fig. 5). Aromatic hydrocarbon degradation genes belonging to MAGs of *Thioclava* and *Aestuuriibacter* were found across all experimental treatments while genes from *Neptuniibacter* were abundant only in the oil-only treatment. As expected, all of these MAGs also contained genes involved in the degradation of fatty acids; however, MAGs of *Alteromonas* and *Methylophaga* appeared to serve a significant function primarily in fatty acid degradation which includes the later steps of alkane oxidation (Fig. 5).

By day 6, there was a notable reduction in hydrocarbon degradation potential in the seawater control treatment. However, the number of hydrocarbon degradation genes in both oil-amended treatments increased from day 3, primarily due to an increased abundance in MAGs of *Marinobacter* and *Erythrobacter* in the oil-only and *Alcanivorax* in the oil-plus-dispersant treatments (Fig. 5). Genes involved in the degradation of alkanes were more numerous in the oil-plus-dispersant treatment compared to the oil-only treatment and were mostly associated with MAGs of *Alcanivorax*. On the other hand, the oil-only treatment had a larger amount of aromatic degradation genes that were primarily related to MAGs of *Marinobacter*. On day 15, when hydrocarbon degradation potential was at its lowest in all treatments, *Marinobacter* and *Alcanivorax* remained the primary hydrocarbon degraders in the two oil-amended treatments.

## DISCUSSION

We sought to evaluate the importance of microaggregates after oil spills and determine if their presence may influence hydrocarbon degradation activity in the water column. Microaggregates have been reported in multiple experimental studies (1, 8–10) and were found in freshly collected surface seawater from the Gulf of Mexico. Although these microaggregates do not need oil to form, in the only previous study where they were quantified, they were shown to be more abundant with increasing oil concentrations (10), and other studies show they often have droplets of oil



incorporated into their structure when present (7, 27, 28). However, prior to the current study, whether these BOMAs might play a significant role in the natural biodegradation of spilled oil in the ocean was unexamined.

**BOMA abundance coincides with increased hydrocarbon degradation rates.**

Several hydrocarbon-degrading bacteria and eukaryotes produce exopolymeric substances and other biosurfactants in response to the presence of oil as a mechanism to help solubilize and degrade these compounds (7, 15, 29, 30). This can enhance aggregate formation around oil droplets and may have contributed to the large number of BOMAs observed in the oil-amended treatments in this and similar studies. The addition of dispersant which also acts to solubilize hydrocarbons and increases the abundance of smaller oil droplets in the water column may have further amplified this effect (21, 23). Indeed, more BOMAs were formed in the treatment amended with dispersed oil than in that amended with oil alone (Fig. 1A). This trend was also observed in several previous experiments conducted by our research consortium (see Fig. S7 in the supplemental material) (19), indicating that chemical dispersants do not negatively impact the formation of the small-scale aggregates examined in this study but rather emphasize the connection between the abundance of BOMAs and the presence of oil in the water column.

We utilized a radiotracer-based method to quantify the biological oxidation rates of hexadecane and naphthalene during our experiment. The highest oxidation rates for both compounds occurred in the oil-amended treatments around the same time that the abundance of BOMAs was greatest (e.g., days 3 to 4) (Fig. 1). This evidence supports a linkage between the formation of BOMAs and hydrocarbon degradation. It also indicates that the rates of hydrocarbon degradation in BOMAs may be important in comparison to rates among free-living microorganisms. These findings are the first to link BOMAs to hydrocarbon degradation and are consistent with research showing marine snow and other biomass aggregates are hot spots for microbial activity (28, 31–33).

**BOMAs are distinct from MOS.** While we did find evidence that BOMAs are an important site for hydrocarbon degradation in the marine water column, it remains unclear if BOMAs are a precursor to MOS and the widely reported MOSSFA event that was responsible for transporting up to 31% of oil back to the seafloor following the DwH spill (7, 11–14). Although the number of the microaggregates in our experiment fluctuated over time and with treatment, their overall size did not (Fig. S3). This trend was observed across multiple mesocosm experiments conducted by our research consortium with different seawater sources, nutrient concentrations, and oil/dispersant treatments (Fig. S8) (10, 25, 33). This also suggests BOMAs are a separate phenomenon from larger MOS particles—which in contrast have been demonstrated to coalesce and increase in size over time (28). Our interpretation, however, is complicated by our observation of visible MOS particles cooccurring with microaggregates in our experiments. One possible scenario that resolves this apparent conflict is that BOMAs and MOS particles represent different-size spectra of the same phenomenon. In such a case, our observations indicate a steady-state scenario wherein microaggregates grew larger or stuck together and subsequently sank out over time as MOS while new, smaller microaggregates were formed. However, we cannot rule out that BOMAs and MOS particles are unrelated to one another and BOMAs instead remain small and eventually degrade or disperse into the water column. While both these scenarios merit further study, in either case, BOMAs represent a natural and fundamental component of the microbial response to hydrocarbon exposure which until now has been largely overlooked and underestimated.

**BOMAs are enriched with microorganisms capable of hydrocarbon degradation.**

To determine the role BOMAs serve in the biodegradation of oil spills, we utilized size fractionation to specifically target and identify members of the microbial community present in microaggregates and evaluate their potential to degrade hydrocarbons. Within the first few days, the addition of oil and dispersant initiated a rapid growth of putative hydrocarbon-degrading taxa (2, 3). These included the alkane degrader *Oleibacter* (34) and members of the polycyclic aromatic hydrocarbon (PAH)-

degrading *Cycloclasticus*, *Neptuniibacter*, and *Alteromonas* genera (35, 36). Also abundant were ASVs of *Marinobacter*, *Alcanivorax*, and *Pseudomonas*, of which cultured representatives have been shown to degrade a wide range of hydrocarbon compounds (17, 37, 38). All of these taxa were present in the free-living fraction; however, most were shown to be statistically more abundant in the microaggregates based on our analysis of ASVs (Fig. 2 and 3 and Fig. S5). Additionally, most of these taxa have been seen in other microbiological surveys following oil spill events, including that of DWH, and are frequently identified as critical members involved in the natural response to hydrocarbon pollution (1–6). The prevalence of such organisms in BOMAs further highlights the significant role that aggregated microbial consortia likely serve in hydrocarbon degradation.

Analysis of the size-fractionated ASV data implies there is an aggregate-specific microbial community distinct from that found in the background seawater. Highly abundant taxa in seawater such as “*Candidatus Nitrosopumilus*” and OM43 were very rare or absent in the aggregated communities (Fig. S5). Furthermore, individual ASVs of *Alcanivorax* and *Pseudomonas* exhibited niche separation, showing a distinct preference for either aggregated (ASVs 1, 31, 60, and 401) or free-living (ASVs 12 and 56) lifestyles. It should also be noted that many of the taxa present in BOMAs (e.g., *Alcanivorax*, *Marinobacter*, *Pseudomonas*, *Pseudoalteromonas*, and *Alteromonas*) have been shown to produce exopolymeric substances and associated biosurfactants in the presence of oil, which promotes aggregation (4, 13, 39). Together, this suggests that BOMAs are formed and maintained by a selective group of microorganisms.

Of those taxa that were found to be prevalent in microaggregates in our ASV analysis (Fig. 3), many showed the genetic potential to degrade various hydrocarbon compounds based on a metagenomic analysis of the  $>3.0\text{-}\mu\text{m}$  size fraction (Fig. 5). Early in the experiment (day 3), all treatments showed comparable abundances of hydrocarbon degradation genes, including the seawater control. This was not unexpected given that oil is continually introduced into the Gulf of Mexico through natural seeps and spills of various sizes (40), and putative hydrocarbon-degrading microorganisms (e.g., *Pseudomonas*, *Alteromonas*, *Alcanivorax*, and *Rhodobacteraceae*) were abundant in the freshly collected seawater used to establish the mesocosms. However, without the addition of new oil, the abundance of hydrocarbon degradation genes rapidly declined in the seawater control treatment.

We detected a higher abundance of genes needed for the degradation of aromatic hydrocarbons in the oil-only treatment than in oil plus dispersant. This is in agreement with the higher rates of naphthalene oxidation measured in the oil-only treatment and with the compositional analysis of individual hydrocarbon compounds in our mesocosms, which revealed that the concentration of total PAHs, including naphthalene, was also higher in the oil-only samples (24). The majority of these genes were recovered from MAGs of *Marinobacter* and *Neptuniibacter*, PAH-degrading taxa that showed a preference for the oil-only treatment (Fig. 4; Fig. S5). Conversely, genes involved in the degradation of alkanes were more abundant in the oil-plus-dispersant treatment and largely associated with *Alcanivorax* and *Pseudomonas*. These data are again in agreement with the slightly higher concentrations of total *n*-alkanes measured at the start of the experiment in the oil-plus-dispersant treatment than in oil alone (24). Overall, these results indicate that the changes in the structure of the BOMA community, and thus their ability to degrade specific hydrocarbons, were shaped by the initial availability of individual hydrocarbon compounds (e.g., *n*-alkanes versus PAHs). This variability observed in the composition of the hydrocarbons between the oil-only and oil-plus-dispersant treatments may be attributed to the addition of dispersant, which has been shown to influence the amount of different hydrocarbon compounds accommodated into seawater (24, 41) as well as the biological outcome (9, 10).

In the second half of our experiment, as the total hydrocarbon concentrations and rates of oxidation decreased (Fig. 1), so too did the abundance of BOMAs and hydrocarbon-degrading microorganisms. These taxa were replaced by members of

*Flavobacteriaceae*, *Roseibacillus*, *Loktanella*, *Pseudohongiella*, and *Ruegeria*, many of which exhibit heterotrophic lifestyles not specifically associated with oil degradation (Fig. 2 and Fig. S5) (42–45). Such organisms may be utilizing the degradation products of the hydrocarbons (29), the nutrient-rich EPS of the aggregates (32), or other cellular components. Indeed, high rates of polysaccharide degradation by heterotrophic species following the formation of oil aggregates have been observed in several studies (e.g., references 31 and 32) and were also observed during this experiment (33). This shift toward secondary consumers marks a successional cascade in the aggregated microbial community following the initial degradation of hydrocarbons and may serve as an indicator of oil spill recovery.

**Conclusion.** The large oil-associated aggregates that formed following the DwH spill event were identified as a key factor influencing the transport of hydrocarbons from surface waters to the seafloor. However, the potential for these aggregated microorganisms to influence the degradation of the incorporated oil droplets was poorly understood. The evidence presented in this study reveals that bacterially dominated micrometer-scale aggregates are enriched in hydrocarbon-degrading taxa and primed to utilize a wide range of hydrocarbon compounds. Although it remains unknown if the BOMAs studied here eventually coalesce with time and seed MOS formation, the work presented here indicates BOMAs are an important and fundamental aspect of how microorganisms respond to marine oil spills and provides a previously overlooked mechanism for hydrocarbon degradation in the water column. Given their abundance following oil spills, it is possible that BOMAs also occur in other environments where hydrocarbons are released into the water column, such as at methane seeps and hydrothermal vents. Consequently, the efficiency with which such aggregated microbial consortia degrade hydrocarbons or certain components of oil compared to free-living cells is critical to determining the lifetime of hydrocarbons in the ocean and remains unconstrained.

## MATERIALS AND METHODS

**Experimental design.** In May 2017, surface seawater was collected from the coastal Northern Gulf of Mexico (29°27' N; 94°81' W) and used to establish a mesocosm-scale experiment (100 liters) with three treatments: (i) natural seawater, (ii) seawater amended with Macondo surrogate crude oil (oil-only), and (iii) seawater amended with chemically dispersed oil (oil plus dispersant; see reference 33). The oil treatment was generated by mixing 25 ml of Macondo surrogate crude oil with 130 liters freshly collected seawater for 4 h using a 170-liter baffled recirculating tank (46). This material was then divided into three 100-liter replicate tanks. To generate a chemically dispersed oil, 25 ml of Macondo surrogate crude oil and Corexit (20:1) was added to seawater and mixed as described above. This material was then divided and subsequently diluted 10-fold among three tanks to create the oil-plus-dispersant treatment that had oil concentrations consistent with those found in the oil-only treatment as well as those observed during the Deepwater Horizon oil spill event (46). Immediately prior to the start of the experiment, a freshly collected natural phytoplankton mixture was added to each of the tanks (starting biomass, ~2 to 4  $\mu\text{g}/\text{liter}$ ). Details on nutrient concentrations are provided elsewhere (33). Tanks were maintained for 16 days at room temperature on a 12-h light/dark cycle, with 50 to 60  $\mu\text{mol photons m}^{-2} \text{ s}^{-1}$ , and samples were collected into 1-liter polycarbonate bottles from a spigot on the mesocosm tank.

**Estimated oil equivalents.** Every 24 h, 5 to 20 ml of seawater was collected from the spigot and extracted with dichloromethane (DCM) according to the method of Wade et al. (47), as updated in the work of Wade et al. (46). DCM-extractable hydrocarbons (3 ml) were analyzed using a Horiba Aqualog-UV-800 to measure fluorescence at an excitation of 260 nm and an emission of 372 nm. Fluorescence intensity was compared to a standard curve generated from Macondo surrogate oil to determine the estimated oil equivalent (EOE) concentration. At these wavelengths, chlorophyll *a* (chl *a*) and accessory pigments, as well as colored dissolved organic matter, may generate artificially elevated values, so additional controls were used to correct EOE. Student's *t* test was used to determine the significances of differences in oil concentrations between treatments. Additional details about the hydrocarbon composition and degradation rates are provided elsewhere (24).

**Hydrocarbon oxidation rate.** Rates of biological hydrocarbon oxidation were estimated using [1- $^{14}\text{C}$ ]hexadecane and [1- $^{14}\text{C}$ ]naphthalene (American Radiolabeled Chemicals Inc.). During each time point tested, duplicate 1-ml water samples were collected from each of the triplicate mesocosm tanks for each of the three treatments (seawater control, oil-only, and oil-plus-dispersant). To each sample, 100,000 dpm of either  $^{14}\text{C}$ -labeled hexadecane or naphthalene was added. The samples were incubated in an air-tight vial with a carbon dioxide trap consisting of 100 ml of 0.5 mol liter $^{-1}$  KOH for 12 to 24 h before being terminated with the addition of 50  $\mu\text{l}$  of 100% trichloroacetic acid (TCA) injected through the silicone septum cap. The samples were allowed to sit for another 6 h before the traps were removed to allow for maximum absorbance of liberated  $^{14}\text{CO}_2$ . The contents of the traps were transferred to a clean

20-ml scintillation vial, and 10 ml of CytoScint ES (MP Biomedicals) scintillation cocktail was added. Counts were measured for 3 min on a Beckman Coulter liquid scintillation counter. Killed controls were periodically tested throughout the experiment by either pasteurizing the sample at 80°C for 1 h or acidifying the sample to pH  $\leq 2$  prior to the addition of radiolabeled substrate and incubation. Background incorporation detected in controls was subtracted from rates measured in samples. Samples were collected every 24 h for the first 4 days and then every 48 h until the end of the experiment. Student's *t* test was used to determine the significances of differences in rates between treatments.

**Microscopy and image analysis.** To monitor the number of microbial cells and the formation of micrometer-scale aggregates, water was collected from the freshly collected seawater used to establish the mesocosms and from each tank at each time point and preserved with either formalin (2% final concentration) for standard cell counts or paraformaldehyde (2% final concentration) for catalyzed reporter deposition fluorescence *in situ* hybridization (CARD-FISH). The formalin-preserved samples were processed for cell and microaggregate counts as described previously (10). Briefly, samples were stained with 4',6'-diamidino-2-phenylindole (DAPI; 45  $\mu$ M) nucleic acid dye for 10 min and filter concentrated under vacuum onto 0.2- $\mu$ m-pore-size black polycarbonate filters. Filters were then mounted on a glass microscope slide using CitiFluor AF1 antifading mounting solution. The total number of DAPI-stained cells in 10 fields of view was counted using  $\times 1,000$  magnification on a Zeiss fluorescence microscope (Axio Imager M2; Zeiss, Jena, Germany). To quantify the number of cell aggregates in each of the treatments, total aggregates were counted at  $\times 400$  magnification in 10 fields of view per sample on the same DAPI-stained slide used for total cell enumeration. We defined an aggregate as a tight cluster of 10 or more individual cells. These counts are conservative estimates for the number of microaggregates considering it is possible that some microaggregates may have overlapped during filtration and/or slide preparation. We did not observe evidence of this during our counting; however, if it were to have occurred, it would result in fewer microaggregates being counted than were present. A Student *t* test was used to determine the significances of differences in cell and aggregate abundances between treatments.

To determine aggregate size, images were taken of 100 aggregates per treatment per time point tested and the area of each aggregate was manually calculated using ImageJ software. Differences in aggregate size distribution were evaluated using a Tukey *post hoc* analysis.

CARD-FISH samples were incubated at 4°C for 12 to 16 h before being filter concentrated onto a 0.2- $\mu$ m-pore-size white polycarbonate filter and washed twice with 1 volume of phosphate-buffered saline (137 nM NaCl, 2.7 nM KCl, 10 mM Na<sub>2</sub>HPO<sub>4</sub>, 1.8 mM KH<sub>2</sub>PO<sub>4</sub>). The filters were allowed to dry completely and stored at  $-20^{\circ}\text{C}$ . CARD-FISH was performed following the protocols outlined in the work of Pernthaler et al. (48) and Pernthaler and Pernthaler (49). Horseradish peroxidase-modified probe ALT1413 (5'-TTTGAT CCCACTCCCAT) was used to target *Alteromonas*- and *Colwellia*-related species and hybridized with a 40% formamide concentration. A second probe, ALC665 (5'-CGGAAATTCACCTCCCT), was designed using the Probe Design function in ARB against the SILVA v132 small-subunit database to target the most abundant *Alcanivorax* ASV present in this study. The probe specificity was checked with the SILVA probe match and evaluation tool (TestProbe), and the optimum formamide concentration for hybridization (55%) was determined empirically using isolate LSUCC0630 cultured from the northern Gulf of Mexico (50). Alexa Fluor 488-conjugated tyramide was used to visualize probe deposition, and all cells were counterstained with DAPI. The proportion of probe-targeted cells to total cells was determined in 10 fields of view per sample.

**LSUCC0630 isolate cultivation.** Isolate LSUCC0630 was obtained from the LSUCC culture collection. It was isolated from source water collected on a research cruise in the Gulf of Mexico (PE17-02, Lead Chief Scientist Frank Stewart) from Station C6C (lat 28.8687, long  $-90.4785$ ) on 2 August 2016 using a Niskin rosette onboard the RV *Pelican*. The sample was collected from the Niskin bottle at 14 m (temperature 27.32°C, salinity 35.31). For collection, a 1-liter acid-washed and autoclaved Pyrex bottle was filled with Niskin water until overflowing and sealed. Isolation was performed in custom medium according to the work of Henson et al., 2016 (50).

**Molecular biology analysis.** Water samples (200 ml) were collected daily from each tank and first gravity filtered through a 47-mm-diameter, 3.0- $\mu$ m-pore-size Isopore TSTP filter to collect microaggregates. The filtrate was subsequently filtered under vacuum onto a 47-mm-diameter, 0.2- $\mu$ m-pore-size Supor membrane filter to collect free-living cells. Additional water samples were collected from the starting seawater and from each of the oil and oil-plus-dispersant mixing tanks to account for any changes in the microbial community that may have occurred during experimental setup. These samples (200 ml) were filtered directly onto a 47-mm, 0.2- $\mu$ m Supor membrane filter with no prefiltration. All filters were placed into cryovials and immediately preserved at  $-80^{\circ}\text{C}$  until extraction. DNA was extracted from each filter using the FastDNA spin kit for soil (MP Biomedicals) according to the manufacturer's protocol.

For microbial community analysis, the V4 hypervariable region of the 16S rRNA gene was amplified using universal primers 515F and 806R (10, 51) and sequenced on the Illumina MiSeq platform (500 cycle, 250-bp paired end [PE]) at the Georgia Genomics Facility (Athens, GA, USA). Raw 16S rRNA gene sequence reads were curated and coalesced into amplicon sequence variants (ASVs) using the standard pipeline of the DADA2 R package (52). All ASVs were subsampled to an even depth before downstream ecological analyses were performed with mothur (53) or the R packages phyloseq (54) and vegan (55). Changes in microbial community structure between treatments and over time were examined using nonmetric multidimensional scaling (NMDS) based on a Bray-Curtis dissimilarity index and tested for significance using analysis of molecular variance (AMOVA) (56). To evaluate which individual ASVs differentiated the microbial communities found on the 0.2- to 3.0- $\mu$ m and  $>3.0$ - $\mu$ m filter size fractions in each treatment and at each time point, a linear discriminant analysis (LDA) combined with effect size measurements (26) was used. Significance of differential abundance was based on a *P* value of  $<0.05$  in the Kruskal-Wallis test and a score of  $\geq 2.0$  in pairwise Wilcoxon tests.

For metagenomic analysis, DNA extracted from the 3.0- $\mu$ m filters from three representative time points (days 3, 6, and 15) was sequenced on the Illumina HiSeq platform (100-bp PE) at the University of Delaware DNA Sequencing & Genotyping Center (Newark, DE, USA). DNA from triplicate tanks was pooled in equimolar concentration and treated as a single sample for sequencing. Raw reads were trimmed and filtered for quality using Trimmomatic (average quality = 30, minimum length = 75) (57). All samples were pooled, assembled with IDBA-UD (58), and binned with MaxBin2 (59) using default parameters. Individual sequence reads from each sample were then mapped to the binned contigs using Bowtie2 (60) to determine coverage across samples. Bins were imported into Anvi'o (61) where genes were identified, annotated according to the Kyoto Encyclopedia of Genes and Genomes (KEGG) database, and taxonomically assigned using Kaiju (62) by comparison to the NCBI nr database. Bins were evaluated for completeness and contamination using CheckM (63) and manually refined in Anvi'o. Curated bins with >50% completeness and <10% contamination were retained for further analysis (see Table S1 in the supplemental material). The abundance of bins and genes across samples was determined by evaluating the mapped reads using RPKM (reads per kilobase per million) normalization with the formulation:  $A_{ij} = (N_{ij}/L_i) \times (1/T_j)$ , where  $A_{ij}$  is the abundance of bin  $i$  in sample  $j$ ,  $N_{ij}$  is the number of reads that map to bin  $i$  from sample  $j$ ,  $L_i$  is the length of bin  $i$  in kilobases, and  $T_j$  is the total number of reads in sample  $j$  divided by  $10^6$  as described in reference 64. Genes belonging to a KEGG pathway involved in the degradation of saturated hydrocarbons (alkanes and cycloalkanes), PAHs, or their metabolic intermediates in central metabolism (glycolysis, tricarboxylic acid cycle) were specifically identified and quantified (Table S2) (26, 65).

**Data availability.** Sequences were submitted to the National Center for Biotechnology Information Sequence Read Archive under BioProject [PRJNA629337](https://www.ncbi.nlm.nih.gov/bioproject/PRJNA629337) (metagenomes) and BioProject [PRJNA623576](https://www.ncbi.nlm.nih.gov/bioproject/PRJNA623576) (16S rRNA amplicons). Data are publicly available through the Gulf of Mexico Research Initiative Information and Data Cooperative (GRIIDC) at <http://data.gulfresearchinitiative.org> (DOIs: <https://doi.org/10.7266/3ZVPZ2F8>, <https://doi.org/10.7266/n7-z8x6-km14>, <https://doi.org/10.7266/N71GNKT1>, <https://doi.org/10.7266/n7-v9q1-5116>, and <https://doi.org/10.7266/n7-1kx8-0z36>).

## SUPPLEMENTAL MATERIAL

Supplemental material is available online only.

**FIG S1**, EPS file, 0.9 MB.

**FIG S2**, EPS file, 0.7 MB.

**FIG S3**, EPS file, 0.8 MB.

**FIG S4**, EPS file, 1.4 MB.

**FIG S5**, EPS file, 1.9 MB.

**FIG S6**, EPS file, 9.1 MB.

**FIG S7**, EPS file, 2.3 MB.

**FIG S8**, EPS file, 4.3 MB.

**TABLE S1**, XLSX file, 0.02 MB.

**TABLE S2**, XLSX file, 0.02 MB.

## ACKNOWLEDGMENTS

This research was made possible by a grant from The Gulf of Mexico Research Initiative to support consortium research entitled ADDOMEx (Aggregation and Degradation of Dispersants and Oil by Microbial Exopolymers) and the ADDOMEx-2 Consortium. This material is based upon work supported in part by the National Science Foundation under grant number NSF OCE-1455851 and NSF OCE-1849932.

Any opinions, findings, and conclusions or recommendations expressed in this material are those of the author(s) and do not necessarily reflect the views of the National Science Foundation.

We declare there are no competing financial interests to disclose.

We offer many thanks to J. C. Thrash and the LSUCC culture collection for supplying isolate LSUCC0630 as well as the Geochemical and Environmental Research Group at Texas A&M University for help with experimental design.

Author contributions: A.M.A., S.M.D., A.Q., and J.B.S. designed research; A.M.A., S.M.D., M.I.M., and C.P.H. performed research; A.M.A., S.M.D., A.Q., and J.B.S. wrote the paper.

## REFERENCES

- Baelum J, Borglin S, Chakraborty R, Fortney JL, Lamendella R, Mason OU, Auer M, Zemla M, Bill M, Conrad ME, Malfatti SA, Tringe SG, Holman H-Y, Hazen TC, Jansson JK. 2012. Deep-sea bacteria enriched by oil and dispersant from the Deepwater Horizon spill. *Environ Microbiol* 14: 2405–2416. <https://doi.org/10.1111/j.1462-2920.2012.02780.x>.
- Hazen TC, Dubinsky EA, DeSantis TZ, Andersen GL, Piceno YM, Singh N, Jansson JK, Probst A, Borglin SE, Fortney JL, Stringfellow WT, Bill M, Conrad ME, Tom LM, Chavarria KL, Alusi TR, Lamendella R, Joyner DC, Spier C, Baelum J, Auer M, Zemla ML, Chakraborty R, Sonnenthal EL, D'haeseleer P, Holman H-YN, Osman S, Lu Z, Van Nostrand JD, Deng Y,

- Zhou J, Mason OU. 2010. Deep-sea oil plume enriches indigenous oil-degrading bacteria. *Science* 330:204–208. <https://doi.org/10.1126/science.1195979>.
3. Redmond MC, Valentine DL. 2012. Natural gas and temperature structured a microbial community response to the Deepwater Horizon oil spill. *Proc Natl Acad Sci U S A* 109:20292–20297. <https://doi.org/10.1073/pnas.1108756108>.
  4. King G, Kostka J, Hazen T, Sobczyk P. 2015. Microbial responses to the Deepwater Horizon oil spill: from coastal wetlands to the deep sea. *Annu Rev Mar Sci* 7:377–401. <https://doi.org/10.1146/annurev-marine-010814-015543>.
  5. Dubinsky EA, Conrad ME, Chakraborty R, Bill M, Borglin SE, Hollibaugh JT, Mason OU, Piceno YM, Reid FC, Stringfellow WT, Tom LM, Hazen TC, Andersen GL. 2013. Succession of hydrocarbon-degrading bacteria in the aftermath of the Deepwater Horizon oil spill in the Gulf of Mexico. *Environ Sci Technol* 47:10860–10867. <https://doi.org/10.1021/es401676y>.
  6. Brooijmans RJ, Pastink MI, Siezen RJ. 2009. Hydrocarbon-degrading bacteria: the oil-spill clean-up crew. *Microb Biotechnol* 2:587–594. <https://doi.org/10.1111/j.1751-7915.2009.00151.x>.
  7. Quigg A, Passow U, Chin W-C, Xu C, Doyle S, Bretherton L, Kamalanathan M, Williams AK, Sylvan JB, Finkel ZV, Knap AH, Schwehr KA, Zhang S, Sun L, Wade TL, Obeid W, Hatcher PG, Santschi PH. 2016. The role of microbial exopolymers in determining the fate of oil and chemical dispersants in the ocean. *Limnol Oceanogr Lett* 1:3–26. <https://doi.org/10.1002/lo.10030>.
  8. Ziervogel K, D'souza N, Sweet J, Yan B, Passow U. 2014. Natural oil slicks fuel surface water microbial activities in the northern Gulf of Mexico. *Front Microbiol* 5:188. <https://doi.org/10.3389/fmicb.2014.00188>.
  9. Kleindienst S, Seidel M, Ziervogel K, Grim S, Loftis K, Harrison S, Malkin SY, Perkins MJ, Field J, Sogin ML, Dittmar T, Passow U, Medeiros PM, Joye SB. 2015. Chemical dispersants can suppress the activity of natural oil-degrading microorganisms. *Proc Natl Acad Sci U S A* 112:14900–14905. <https://doi.org/10.1073/pnas.1507380112>.
  10. Doyle SM, Whitaker EA, De Pascuale V, Wade TL, Knap AH, Santschi PH, Quigg A, Sylvan JB. 2018. Rapid formation of microbe-oil aggregates and changes in community composition in coastal surface water following exposure to oil and the dispersant Corexit. *Front Microbiol* 9:689. <https://doi.org/10.3389/fmicb.2018.00689>.
  11. Daly KL, Passow U, Chanton J, Hollander D. 2016. Assessing the impacts of oil-associated marine snow formation and sedimentation during and after the Deepwater Horizon oil spill. *Anthropocene* 13:18–33. <https://doi.org/10.1016/j.ancene.2016.01.006>.
  12. Burd AB, Chanton JP, Daly KL, Gilbert S, Passow U, Quigg A. 2020. The science behind marine-oil snow and MOSSFA: past, present, and future. *Prog Oceanogr* 187:102398. <https://doi.org/10.1016/j.pocean.2020.102398>.
  13. Passow U, Ziervogel K, Asper V, Diercks A. 2012. Marine snow formation in the aftermath of the Deepwater Horizon oil spill in the Gulf of Mexico. *Environ Res Lett* 7:e035301. <https://doi.org/10.1088/1748-9326/7/3/035301>.
  14. Quigg A, Passow U, Daly KL, Burd A, Hollander DJ, Schwing PT, Lee K. 2020. Marine oil snow sedimentation and flocculent accumulation (MOSSFA) events: learning from the past to predict the future, p 196–220. *In* Murawski SA, Ainsworth CH, Gilbert S, Hollander DJ, Paris CB, Schlüter M, Wetzel DL (ed), *Deep oil spills*. Springer, Cham, Switzerland.
  15. Gutierrez T, Berry D, Yang T, Mishamandani S, McKay L, Teske A, Aitken MD. 2013. Role of bacterial exopolysaccharides (EPS) in the fate of the oil released during the Deepwater Horizon oil spill. *PLoS One* 8:e67717. <https://doi.org/10.1371/journal.pone.0067717>.
  16. Gutierrez T, Mulloy B, Black K, Green DH. 2007. Glycoprotein emulsifiers from two marine *Halomonas* species: chemical and physical characterization. *J Appl Microbiol* 103:1716–1727. <https://doi.org/10.1111/j.1365-2672.2007.03407.x>.
  17. Xu C, Zhang S, Beaver M, Lin P, Sun L, Doyle SM, Sylvan JB, Wozniak A, Hatcher PG, Kaiser K, Yan G, Schwehr KA, Lin Y, Wade TL, Chin W-C, Chiu M-H, Quigg A, Santschi PH. 2018. The role of microbially-mediated exopolymeric substances (EPS) in regulating Macondo oil transport in a mesocosm experiment. *Mar Chem* 206:52–61. <https://doi.org/10.1016/j.marchem.2018.09.005>.
  18. Santschi PH, Xu C, Schwehr KA, Lin P, Sun L, Chin W-C, Kamalanathan M, Bacosa HP, Quigg A. 2020. Can the protein/carbohydrate (P/C) ratio of exopolymeric substances (EPS) be used as a proxy for their 'stickiness' and aggregation propensity? *Mar Chem* 218:103734. <https://doi.org/10.1016/j.marchem.2019.103734>.
  19. Johansson S, Larsson U, Boehm P. 1980. The Tseis oil spill impact on the pelagic ecosystem. *Mar Pollut Bull* 11:284–293. [https://doi.org/10.1016/0025-326X\(80\)90166-6](https://doi.org/10.1016/0025-326X(80)90166-6).
  20. Patton JS, Rigler MW, Boehm PD, Fiest DL. 1981. Ixtoc 1 oil spill: flaking of surface mousse in the Gulf of Mexico. *Nature* 290:235–238. <https://doi.org/10.1038/290235a0>.
  21. Li Z, Lee K, Kepkey PE, Mikkelsen O, Pottsmith C. 2011. Monitoring dispersed oil droplet size distribution at the Gulf of Mexico Deepwater Horizon spill site. *Int Oil Spill Conf Proc*, abstr 377.
  22. Passow U, Sweet J, Quigg A. 2017. How the dispersant Corexit impacts the formation of sinking marine oil snow. *Mar Pollut Bull* 125:139–145. <https://doi.org/10.1016/j.marpolbul.2017.08.015>.
  23. Waldrop MM. 2019. News feature: the perplexing physics of oil dispersants. *Proc Natl Acad Sci U S A* 116:10603–10607. <https://doi.org/10.1073/pnas.1907155116>.
  24. Shi D, Bera G, Knap AH, Quigg A, Al Atwah I, Gold-Bouchot G, Wade TL. 2020. A mesocosm experiment to determine half-lives of individual hydrocarbons in simulated oil spill scenarios with and without the dispersant, Corexit. *Mar Pollut Bull* 151:110804. <https://doi.org/10.1016/j.marpolbul.2019.110804>.
  25. Doyle SM, Lin G, Morales-McDevitt M, Wade TL, Quigg A, Sylvan JB. 2020. Niche partitioning between coastal and offshore shelf waters results in differential expression of alkane and PAH catabolic pathways. *mSystems* 5:e00668-20. <https://doi.org/10.1128/mSystems.00668-20>.
  26. Segata N, IZard J, Waldron L, Gevers D, Miropolsky L, Garrett WS, Huttenhower C. 2011. Metagenomic biomarker discovery and explanation. *Genome Biol* 12:R60. <https://doi.org/10.1186/gb-2011-12-6-r60>.
  27. Hatcher PG, Obeid W, Wozniak AS, Xu C, Zhang S, Santschi PH, Quigg A. 2018. Identifying oil/marine snow associations in mesocosm simulations of the Deepwater Horizon oil spill event using solid-state <sup>13</sup>C NMR spectroscopy. *Mar Pollut Bull* 126:159–165. <https://doi.org/10.1016/j.marpolbul.2017.11.004>.
  28. Henry IA, Netzer R, Davies EJ, Brakstad OG. 2020. Formation and fate of oil-related aggregates (ORAs) in seawater at different temperatures. *Mar Pollut Bull* 159:111483. <https://doi.org/10.1016/j.marpolbul.2020.111483>.
  29. Head IM, Jones DM, Röling WF. 2006. Marine microorganisms make a meal of oil. *Nat Rev Microbiol* 4:173–182. <https://doi.org/10.1038/nrmicro1348>.
  30. Passow U. 2016. Formation of rapidly-sinking, oil-associated marine snow. *Deep Sea Res 2 Top Stud Oceanogr* 129:232–240. <https://doi.org/10.1016/j.dsr2.2014.10.001>.
  31. Ziervogel K, Joye SB, Kleindienst S, Malkin SY, Passow U, Steen AD, Arnosti C. 2019. Polysaccharide hydrolysis in the presence of oil and dispersants: insights into potential degradation pathways of exopolymeric substances (EPS) from oil-degrading bacteria. *Elem Sci Anthropol* 7:31. <https://doi.org/10.1525/elementa.371>.
  32. Arnosti C, Ziervogel K, Yang T, Teske A. 2016. Oil-derived marine aggregates—hot spots of polysaccharide degradation by specialized bacterial communities. *Deep Sea Res 2 Top Stud Oceanogr* 129:179–186. <https://doi.org/10.1016/j.dsr2.2014.12.008>.
  33. Kamalanathan M, Doyle SM, Xu C, Achberger AM, Wade TL, Schwehr K, Santschi PH, Sylvan JB, Quigg A. 2020. Exoenzymes as a signature of microbial response to marine environmental conditions. *mSystems* 5:e00290-20. <https://doi.org/10.1128/mSystems.00290-20>.
  34. Teramoto M, Ohuchi M, Hatmanti A, Darmayati Y, Widyastuti Y, Harayama S, Fukunaga Y. 2011. *Oleibacter marinus* gen. nov., sp. nov., a bacterium that degrades petroleum aliphatic hydrocarbons in a tropical marine environment. *Int J Syst Evol Microbiol* 61:375–380. <https://doi.org/10.1099/ijs.0.018671-0>.
  35. Jin HM, Kim JM, Lee HJ, Madsen EL, Jeon CO. 2012. *Alteromonas* as a key agent of polycyclic aromatic hydrocarbon biodegradation in crude oil-contaminated coastal sediment. *Environ Sci Technol* 46:7731–7740. <https://doi.org/10.1021/es3018545>.
  36. Dombrowski N, Donaho JA, Gutierrez T, Seitz KW, Teske AP, Baker BJ. 2016. Reconstructing metabolic pathways of hydrocarbon-degrading bacteria from the Deepwater Horizon oil spill. *Nat Microbiol* 1:16057. <https://doi.org/10.1038/nmicrobiol.2016.57>.
  37. Jiménez N, Viñas M, Guiu-Aragón C, Bayona JM, Albaigés J, Solanas AM. 2011. Polyphasic approach for assessing changes in an autochthonous marine bacterial community in the presence of Prestige fuel oil and its biodegradation potential. *Appl Microbiol Biotechnol* 91:823–834. <https://doi.org/10.1007/s00253-011-3321-4>.
  38. Wu T, Xu J, Xie W, Yao Z, Yang H, Sun C, Li X. 2018. *Pseudomonas aeruginosa* L10: a hydrocarbon-degrading, biosurfactant-producing, and plant-growth-promoting endophytic bacterium isolated from a reed (*Phragmites australis*). *Front Microbiol* 9:1087. <https://doi.org/10.3389/fmicb.2018.01087>.

39. Ennouri H, d'Abzac P, Hakil F, Branchu P, Naïtali M, Lomenech AM, Oueslati R, Desbrières J, Sivadon P, Grimaud R. 2017. The extracellular matrix of the oleolytic biofilms of *Marinobacter hydrocarbonoclasticus* comprises cytoplasmic proteins and T2SS effectors that promote growth on hydrocarbons and lipids. *Environ Microbiol* 19:159–173. <https://doi.org/10.1111/1462-2920.13547>.
40. MacDonald IR, Garcia-Pineda O, Beet A, Daneshgar Asl S, Feng L, Graettinger G, French-McCay D, Holmes J, Hu C, Huffer F, Leifer I, Muller-Karger F, Solow A, Silva M, Swayze G. 2015. Natural and unnatural oil slicks in the Gulf of Mexico. *J Geophys Res Oceans* 120:8364–8380. <https://doi.org/10.1002/2015JC011062>.
41. Couillard CM, Lee K, Légaré B, King TL. 2005. Effect of dispersant on the composition of the water-accommodated fraction of crude oil and its toxicity to larval marine fish. *Environ Toxicol Chem* 24:1496–1504. <https://doi.org/10.1897/04-267r.1>.
42. Lau SC, Tsoi MM, Li X, Plakhotnikova I, Wu M, Wong P-K, Qian P-Y. 2004. *Loktanella hongkongensis* sp. nov., a novel member of the  $\alpha$ -Proteobacteria originating from marine biofilms in Hong Kong waters. *Int J Syst Evol Microbiol* 54:2281–2284. <https://doi.org/10.1099/ijs.0.63294-0>.
43. Yoon J, Matsuo Y, Adachi K, Nozawa M, Matsuda S, Kasai H, Yokota A. 2008. Description of *Persicirhabdus sediminis* gen. nov., sp. nov., *Roseibacillus ishigakijimensis* gen. nov., sp. nov., *Roseibacillus ponti* sp. nov., *Roseibacillus persicus* sp. nov., *Luteolibacter pohnpensis* gen. nov., sp. nov. and *Luteolibacter algae* sp. nov., six marine members of the phylum 'Verrucomicrobia', and emended descriptions of the class Verrucomicrobiae, the order Verrucomicrobiales and the family Verrucomicrobiaceae. *Int J Syst Evol Microbiol* 58:998–1007. <https://doi.org/10.1099/ijs.0.65520-0>.
44. Rivers AR, Smith CB, Moran MA. 2014. An updated genome annotation for the model marine bacterium *Ruegeria pomeroyi* DSS-3. *Stand Genomic Sci* 9:11. <https://doi.org/10.1186/1944-3277-9-11>.
45. Xu L, Wu Y-H, Jian S-L, Wang C-S, Wu M, Cheng L, Xu X-W. 2016. *Pseudohongiellanitratireducens* sp. nov., isolated from seawater, and emended description of the genus *Pseudohongiella*. *Int J Syst Evol Microbiol* 66:5155–5160. <https://doi.org/10.1099/ijssem.0.001489>.
46. Wade TL, Morales-McDevitt M, Bera G, Shi D, Sweet S, Wang B, Gold-Bouchot G, Quigg A, Knap AH. 2017. A method for the production of large volumes of WAF and CEWAF for dosing mesocosms to understand marine oil snow formation. *Heliyon* 3:e00419. <https://doi.org/10.1016/j.heliyon.2017.e00419>.
47. Wade TL, Sweet ST, Sericano JL, Guinasso NL, Diercks A-R, Highsmith RC, Asper VL, Joung D, Shiller AM, Lohrenz SE. 2011. Analyses of water samples from the Deepwater Horizon oil spill: documentation of the subsurface plume, p 77–82. *In* Lui Y, Macfadyen A, Ji ZG, Weisberg RH (ed), *Monitoring and modeling the Deepwater Horizon oil spill: a record-breaking enterprise*. American Geophysical Union Press, Washington, DC.
48. Pernthaler A, Pernthaler J, Amann R. 2002. Fluorescence in situ hybridization and catalyzed reporter deposition for the identification of marine bacteria. *Appl Environ Microbiol* 68:3094–3101. <https://doi.org/10.1128/AEM.68.6.3094-3101.2002>.
49. Pernthaler A, Pernthaler J. 2007. Fluorescence in situ hybridization for the identification of environmental microbes, p 153–164. *In* Hilario E, Mackay J (ed), *Protocols for nucleic acid analysis by nonradioactive probes*. Humana Press, Totowa, NJ.
50. Henson MW, Pitre DM, Weckhorst JL, Lanclos VC, Webber AT, Thrash JC. 2016. Artificial seawater media facilitate cultivating members of the microbial majority from the Gulf of Mexico. *mSphere* 1:e00124-16. <https://doi.org/10.1128/mSphere.00124-16>.
51. Walters W, Hyde ER, Berg-Lyons D, Ackermann G, Humphrey G, Parada A, Gilbert JA, Jansson JK, Caporaso JG, Fuhrman JA, Apprill A, Knight R. 2016. Improved bacterial 16S rRNA gene (V4 and V4-5) and fungal internal transcribed spacer marker gene primers for microbial community surveys. *mSystems* 1:e00009-15. <https://doi.org/10.1128/mSystems.00009-15>.
52. Callahan BJ, McMurdie PJ, Rosen MJ, Han AW, Johnson AJA, Holmes SP. 2016. DADA2: high-resolution sample inference from Illumina amplicon data. *Nat Methods* 13:581–583. <https://doi.org/10.1038/nmeth.3869>.
53. Schloss PD, Westcott SL, Ryabin T, Hall JR, Hartmann M, Hollister EB, Lesniewski RA, Oakley BB, Parks DH, Robinson CJ, Sahl JW, Stres B, Thallinger GG, Van Horn DJ, Weber CF. 2009. Introducing mothur: open-source, platform-independent, community-supported software for describing and comparing microbial communities. *Appl Environ Microbiol* 75:7537–7541. <https://doi.org/10.1128/AEM.01541-09>.
54. McMurdie PJ, Holmes S. 2013. phyloseq: an R package for reproducible interactive analysis and graphics of microbiome census data. *PLoS One* 8:e61217. <https://doi.org/10.1371/journal.pone.0061217>.
55. Oksanen J, Kindt R, Legendre P, O'Hara B, Stevens MHH, Oksanen MJ. 2007. The vegan package. *Community Ecology Package* 10:631–637.
56. Excoffier L, Smouse PE, Quattro JM. 1992. Analysis of molecular variance inferred from metric distances among DNA haplotypes: application to human mitochondrial DNA restriction data. *Genetics* 131:479–491. <https://doi.org/10.1093/genetics/131.2.479>.
57. Bolger AM, Lohse M, Usadel B. 2014. Trimmomatic: a flexible trimmer for Illumina sequence data. *Bioinformatics* 30:2114–2120. <https://doi.org/10.1093/bioinformatics/btu170>.
58. Peng Y, Leung HC, Yiu S-M, Chin FY. 2012. IDBA-UD: a de novo assembler for single-cell and metagenomic sequencing data with highly uneven depth. *Bioinformatics* 28:1420–1428. <https://doi.org/10.1093/bioinformatics/bts174>.
59. Kang DD, Li F, Kirtan E, Thomas A, Egan R, An H, Wang Z. 2019. MetaBAT 2: an adaptive binning algorithm for robust and efficient genome reconstruction from metagenome assemblies. *PeerJ* 7:e7359. <https://doi.org/10.7717/peerj.7359>.
60. Langmead B, Salzberg SL. 2012. Fast gapped-read alignment with Bowtie 2. *Nat Methods* 9:357–359. <https://doi.org/10.1038/nmeth.1923>.
61. Eren AM, Esen ÖC, Quince C, Vineis JH, Morrison HG, Sogin ML, Delmont TO. 2015. Anvi'o: an advanced analysis and visualization platform for 'omics data. *PeerJ* 3:e1319. <https://doi.org/10.7717/peerj.1319>.
62. Menzel P, Ng KL, Krogh A. 2016. Fast and sensitive taxonomic classification for metagenomics with Kaiju. *Nat Commun* 7:11257–11259. <https://doi.org/10.1038/ncomms11257>.
63. Parks DH, Imelfort M, Skennerton CT, Hugenholtz P, Tyson GW. 2015. CheckM: assessing the quality of microbial genomes recovered from isolates, single cells, and metagenomes. *Genome Res* 25:1043–1055. <https://doi.org/10.1101/gr.186072.114>.
64. Thrash JC, Seitz KW, Baker BJ, Temperton B, Gillies LE, Rabalais NN, Henrissat B, Mason OU. 2017. Metabolic roles of uncultivated bacterioplankton lineages in the northern Gulf of Mexico "Dead Zone." *mBio* 8:e07074-17. <https://doi.org/10.1128/mBio.01017-17>.
65. Seo J-S, Keum Y-S, Li QX. 2009. Bacterial degradation of aromatic compounds. *Int J Environ Res Public Health* 6:278–309. <https://doi.org/10.3390/ijerph6010278>.